



PCCP

Unraveling the structural stability and the electronic structure of ThO₂ nanoclusters

Journal:	<i>Physical Chemistry Chemical Physics</i>
Manuscript ID	CP-ART-01-2020-000478.R1
Article Type:	Paper
Date Submitted by the Author:	28-May-2020
Complete List of Authors:	Aguirre, Néstor; Los Alamos National Laboratory, Theoretical Division Jung, Julie; Los Alamos National Laboratory, Theoretical Division Yang, Ping; Los Alamos National Laboratory, Theoretical Division

SCHOLARONE™
Manuscripts



Cite this: DOI: 10.1039/xxxxxxxxxx

Unraveling the structural stability and the electronic structure of ThO₂ clusters

Néstor F. Aguirre,^{a‡} Julie Jung,^{a‡} and Ping Yang,^{a*}

Received Date

Accepted Date

DOI: 10.1039/xxxxxxxxxx

www.rsc.org/journalname

Unraveling the correlations between the geometry, the relative energy and the electronic structure of metal oxide nanostructures is crucial for a better control of their size, shape and properties. In this work, we investigated these correlations for stoichiometric thorium dioxide clusters ranging from ThO₂ to Th₈O₁₆ using an chemically-driven geometry search algorithm in combination with state-of-the-art first principle calculations. This strategy allows us to homogeneously screen the potential energy surface of actinide oxide cluster for the first time. It is found that the presence of peroxy and superoxy groups tends to increase the total energy of the system by at least 3.5 eV and 7 eV, respectively. For the larger clusters, the presence of terminal oxygen atoms increases the energy by about 0.5 eV. Regarding the electronic structure, it is found that the HOMO-LUMO gap is larger from systems containing bridging oxygen atoms only (~2-3.5 eV) than for systems containing oxo groups (~1-3 eV), peroxy groups (~0-2 eV), and superoxy groups (~0-1 eV). Furthermore, while the LUMO is always dominated by thorium orbitals, the composition of the HOMO changes upon the presence or the absence of oxo, peroxy and/or superoxy groups: in the presence of peroxy groups, it is dominated by thorium orbitals, in all other cases, it is dominated by oxygen orbitals, and rather localized in the presence of terminal oxo or superoxy groups. These correlations are of great interest for synthesizing clusters with tailored properties, especially for applications in the field of nuclear energy and heterogeneous catalysis.

1 Introduction

Thorium dioxide nanomaterials play an increasingly important role in the design of new generations of nuclear fuels, as they are expected to improve both efficiency and safety.¹⁻⁷ More recently, they have also become popular for catalysis applications. Indeed, besides having oxidation states spanning from +II to +IV, thorium is known to have a labile coordination spheres, as a consequence of its large ionic radius, which makes it a good candidate for redox activation processes and addition/subtraction reactions.⁸ In addition, thorium dioxide nanoparticles have also been extensively used as model systems to investigate the transport and migration of early actinide colloids and particles in environmental, biological and geological media.⁹ Yet, despite these broad applications, actinide oxide clusters have not, to date, undergone the same interest as transition metal based clusters.^{8,10-20}

In that context, the purpose of the present work is to evidence and rationalize correlations between the geometry, the relative energy and the electronic structure of thorium dioxide stoichiometric clusters ranging from ThO₂ to Th₈O₁₆, hence addressing a pressing need to better understand actinide oxide clusters.

From a computational perspective, the challenge is twofold: On the one hand, make sure that the electronic structure of the clusters is described accurately,^{21,22} and on the other hand, make sure that the potential energy surface is screened in an affordable but thorough way. The latter point is particularly challenging as the number and the density of stable configurations increase exponentially with the size of the system,²³ which makes the determination of lowest energy structures even more complicated. Herein, this is achieved by combining density functional theory (DFT) calculations with a new type of chemically-driven geometry search algorithm (ESI†, Section S1). The complexity of the problem is further raised by the presence of thorium, which, as most actinide elements, is known for having a rather intricate electronic structure:²⁴⁻²⁷ in addition to the intrinsic multireference character of their wave function, which stems from the presence of unpaired electrons in their 5f and 6d shells, and from the strong contribution of spin-orbit coupling, actinides also have multiple stable oxidation states. Hence, from the computational perspective, these effects can be quite expensive and challenging to describe accurately.^{11,19,28-33}

This manuscript is organized as follows. First, the generation

[‡] NFA and JJ contributed equally; ^a Theoretical Division, Los Alamos National Laboratory, Los Alamos, New Mexico 87545, United States; * E-mail: pyang@lanl.gov

† Electronic Supplementary Information (ESI) available: Computational details, structures and supplementary figures and tables. See DOI: 10.1039/b000000x/

of the clusters by the new search algorithm is discussed. Second, the stabilization energy across the cluster series (Th_nO_{2n} with $n = 1 - 8$), as well as the structural and electronic features of the lowest energy structures, are examined. Third, for each set of clusters, the relative energy and the electronic structure are examined with respect to the presence or absence of different structural features, giving us insight into the structural features stabilizing ThO_2 clusters. Finally, the aforementioned correlations are discussed in the context of chemistry, as potential guideline to achieve clusters with desired properties for dedicated applications.

2 Results and discussion

2.1 Geometry search

The set of structures used to evidence correlations between the geometry, the relative energy and the electronic structure of thorium dioxide clusters ranging from ThO_2 to Th_8O_{16} has been generated using a two-step chemically-driven procedure. This approach is chemically-driven in the sense that the elementary units used to build the clusters are entire ThO_2 molecules. This choice is motivated by the infra-red study of thorium oxide species by Andrews *et al.* as it shows that stoichiometric ThO_2 clusters are predominantly formed in an oxygen-rich conditions. First, an initial set of structures is generated using the stochastic Markov chain strategy, in which an ensemble of transformations (e.g. rotations, translations and substitutions) is applied repeatedly to an ensemble of building-blocks.³⁴ Herein, the building blocks (or units) are either thorium and oxygen atoms, or entire thorium dioxide molecules. For the Th_nO_{2n} clusters with $n = 1 - 4$, simple atoms are used as building blocks. For the clusters with $n = 4 - 5$, ThO_2 monomer units are used, which correspond to the three ThO_2 isomers identified as minima from our own search and published literature^{25,35-41}. Finally, a nucleation inspired approach is used for $n = 6 - 8$, where new initial structures are now built by adding one ThO_2 unit to the low energy structures of the $\text{Th}_{(n-1)}\text{O}_{2(n-1)}$ series. More details are available in the ESI, Section S1.1. At this point, 3000, 15000, and 30000 possible structures are generated for the thorium dioxide clusters Th_nO_{2n} with ($n = 1$), ($n = 2 - 4$)

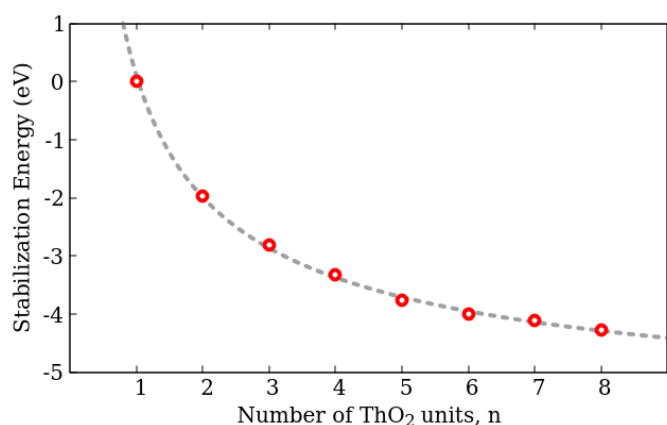


Fig. 1 Stabilization energy of the lowest energy structures, fitted by the equation $SE(n) = 4.65n^{-2/3} + 1.79n^{-1/3} - 6.35^*$ (dashed line)

and ($n = 5 - 8$), respectively. Then, after each series of transformations (or iteration), the proposed structures are checked against atomic positions, to ensure that they do not contain disconnected fragments or superimposed atoms. No objective/loss function was used for screening during the searching process. For a large enough number of iterations (typically on the order of 10^3 iterations), this strategy has been shown to uniformly sample the conformation space.³⁴ During this stage, about 30% to 40% of the structures are removed from the initial set, for each size of cluster. In the present work, this first step is achieved using the M_3C software package.³⁴ In the second step, each structure generated is optimized at the DFT level of theory (ESI†, Section S1.2). After optimization, the duplicated geometries and non-minimum structures, which are characterized by imaginary frequencies, are further screened out of the final dataset. In the end, the two-step geometry search yields a total of 2206 stable structures including global and local energy minima. These structures form the ensemble on which the present work is based (ESI† geometries- Th_nO_{2n} .zip). Their distribution in terms of cluster size is shown in Figure S1 of the ESI†.

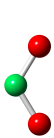
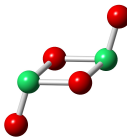
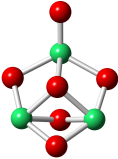
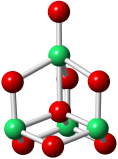
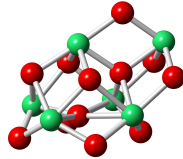
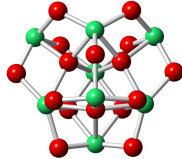
2.2 Geometry and electronic structure of the lowest energy clusters

As the size of the cluster increases, the stabilization energy[¶] of the identified lowest energy structure decreases smoothly following a quadratic dependence on the inverse of the particle size (Figure 1). This trend has also been observed for other metal oxide clusters such as ZnO , MgO , CuO , TiO_2 , and FeTiO_3 ^{42,43}, and it is attributed to the nontrivial contributions of the second-nearest neighbor, and higher-order interactions to the cluster energies. This smooth decrease indicates that, for each size of cluster, the identified lowest energy isomer is either is or very close to the global minimum energy surface (or very close to it). This observation is of prime importance as it confirms the relevance of the dataset, but also the accuracy of the lowest energy structures. Furthermore, the stabilization energy converge to -6.4 eV, which is larger than the stabilization energy of the bulk material^{||} (-7.6 eV).¹¹ This is the sign of upcoming phase transition(s) for larger clusters. A similar behavior has been observed for ZnO nanoclusters.⁴⁴ In fact, for ThO_2 , nanocrystals as small as 5 nm with the same fluorite structure as the bulk have been successfully synthesized by Hudry *et al.*,⁴⁵ while clusters as large as 1 nm were evidenced as stable in the present work (in the Th_8O_{16} series). This observation suggests that the aforementioned phase transition should happen within next 10-15 ThO_2 unit additions. Since no continuous symmetry pattern could be evidenced in the present clusters, it is expected that the phase transition will happen between amorphous and crystalline (fluorite) phases.

¶ The stabilization energy $SE(n)$ is defined as $SE(n) = E(n)/n - E(1)$, with $E(n)$, the total energy of the considered cluster, n , the number of ThO_2 units contained in the cluster, and $E(1)$, the total energy of the global minimum of single unit ThO_2 molecule.

|| The stabilization energy for the ThO_2 bulk material was obtained as $E_{\text{bulk}}/4 - E_{\text{ThO}_2}$, with E_{bulk} , being E_{bulk} and E_{ThO_2} the total energy of the bulk and the single unit of ThO_2 respectively. The unit cell of the ThO_2 bulk includes 4 units of ThO_2 .

Table 1 Molecular structure, symmetry, and range of Th-O bond distances (in Å) for the lowest energy structure of each series of clusters (values in brackets correspond to the next singlet isomers, which are described into more details in the ESI†). Energy difference with the next stable singlet isomer (ΔE in eV), and with the next stable triplet isomer (ΔE_{S-T} in eV) are provided as well.

n	1	2	3	4	5	6	7	8
Structure								
Symmetry	C_{2v}	C_{2h}	C_s	C_{3v}	C_{4v}	C_s	C_1	C_s
d_{Th-O}	1.92	1.92-2.18	1.92-2.39	1.92-2.46	1.93-2.44	2.15-2.62	2.11-2.52	2.14-2.53
ΔE	5.12	0.12	0.62	0.01 [0.06]	0.24	0.32	0.00(4) [0.06]	0.48
ΔE_{S-T}	2.28	2.99	2.75	2.65	2.83	3.21	3.29	3.26

Despite the exponential increase of the number of local minima structures with increasing cluster size,²³ the lowest energy structures are rather well isolated from higher energy structures (Table 1). For Th_nO_{2n} with $n=1,3,5,6$ and 8, the next stable isomer is found at least 0.2 eV higher in energy than the lowest energy structure. For Th_nO_{2n} with $n=2$, this energy is slightly smaller (0.12 eV), but still quantifiable. This suggests that the lowest energy structures of the aforementioned clusters are, for a fact, the lowest energy structures, and that they could be isolated experimentally. For Th_nO_{2n} with $n=4$ and 7, the lowest energy structure and the next two isomers are almost degenerate. This suggest that several structures may be in a thermal equilibrium. Additionally, all these singlet clusters are rather well isolated from their lowest triplet isomers, which are always found at least 2.2 eV higher in energy (Table 1). This is further supported by additional DFT and coupled cluster all electron calculations (ESI†, section S2). Because of this large energy difference, the present work only focuses on the singlet structures. Indeed, it is highly unlikely that such high-energy triplet structures can be stabilized together with the lowest singlet isomer. For that reason, the present work focuses on singlet isomers only.

From a structural perspective (Table 1 and ESI†, section S4), while the lowest energy structures of the Th_nO_{2n} clusters with $n = 1 - 5$ all contain at least one oxygen atom in a terminal position, the one with $n = 6 - 8$ do not. This is most likely the consequence of not having enough thorium atoms to bridge all the oxygen atoms in the smaller clusters. This observation correlates well with the distribution of the Th-O bond distances, which become narrower for the Th_nO_{2n} clusters with $n = 6 - 8$, because the Th-O bond distances are shorter for oxygen atoms in terminal position than for oxygen atoms in bridging position. Furthermore, while some structures have rather high symmetry (C_{2v} , C_{2h} , C_{3v} and C_{4v} for Th_nO_{2n} with $n=1, 2, 4$ and 5 respectively), the others have rather low symmetry (C_s for Th_nO_{2n} with $n=3, 6$ and 8 respectively, and C_1 for Th_nO_{2n} with $n=7$). These values are in good agreement with previous studies.^{25,36-41}

The presence of terminal oxygen atoms is also visible from the

features of the density of states (ESI†, Figure 2 and Table S5). For the clusters with $n=1-5$, the O-2p orbitals of the terminal oxygen atom(s) are the ones that make the largest contribution to the valence orbitals. When the terminal oxygen atoms vanish (i.e. from Th_5O_{10} to Th_6O_{12}) so does their contribution to the DOS, and the HOMO-LUMO gap opens up by about 1 eV. The O-2p orbitals of the oxygen atoms bridging thorium atoms are now the one that make the largest contribution to the valence orbitals at the Fermi level (Figure 2). In all clusters, the largest contribution to the virtual orbitals above the Fermi level comes from the Th-7s. Notably, the HOMO-LUMO gap of these global minima ranges from 2.18 eV up to 3.34 eV (see Table S5), which is significantly smaller than the bulk fluorite material (4.38 eV¹¹). This difference is most likely related to the phase transition discussed earlier, in connection with the asymptotic behavior of the stabilization energy (i.e. stabilization energy not converging towards the bulk limit in Figure 1).

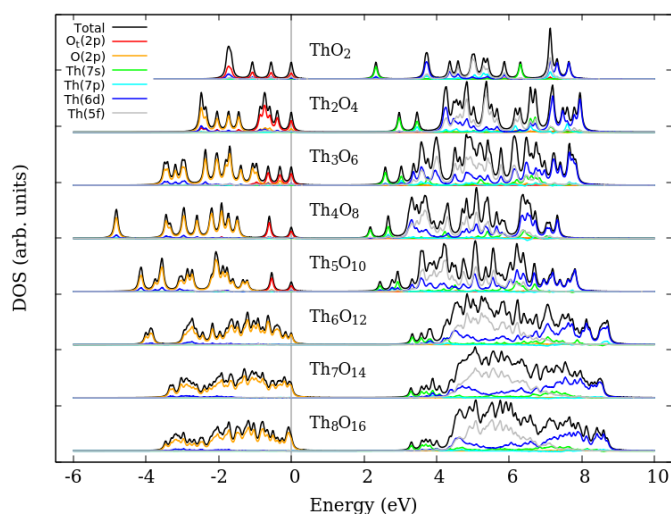


Fig. 2 Total (black) and projected (color) density of states for the lowest energy structure of each cluster ranging from ThO_2 to Th_8O_{16} ($O_t(2p)$ corresponds to the $O(2p)$ of the oxygen atom(s) in terminal positions)

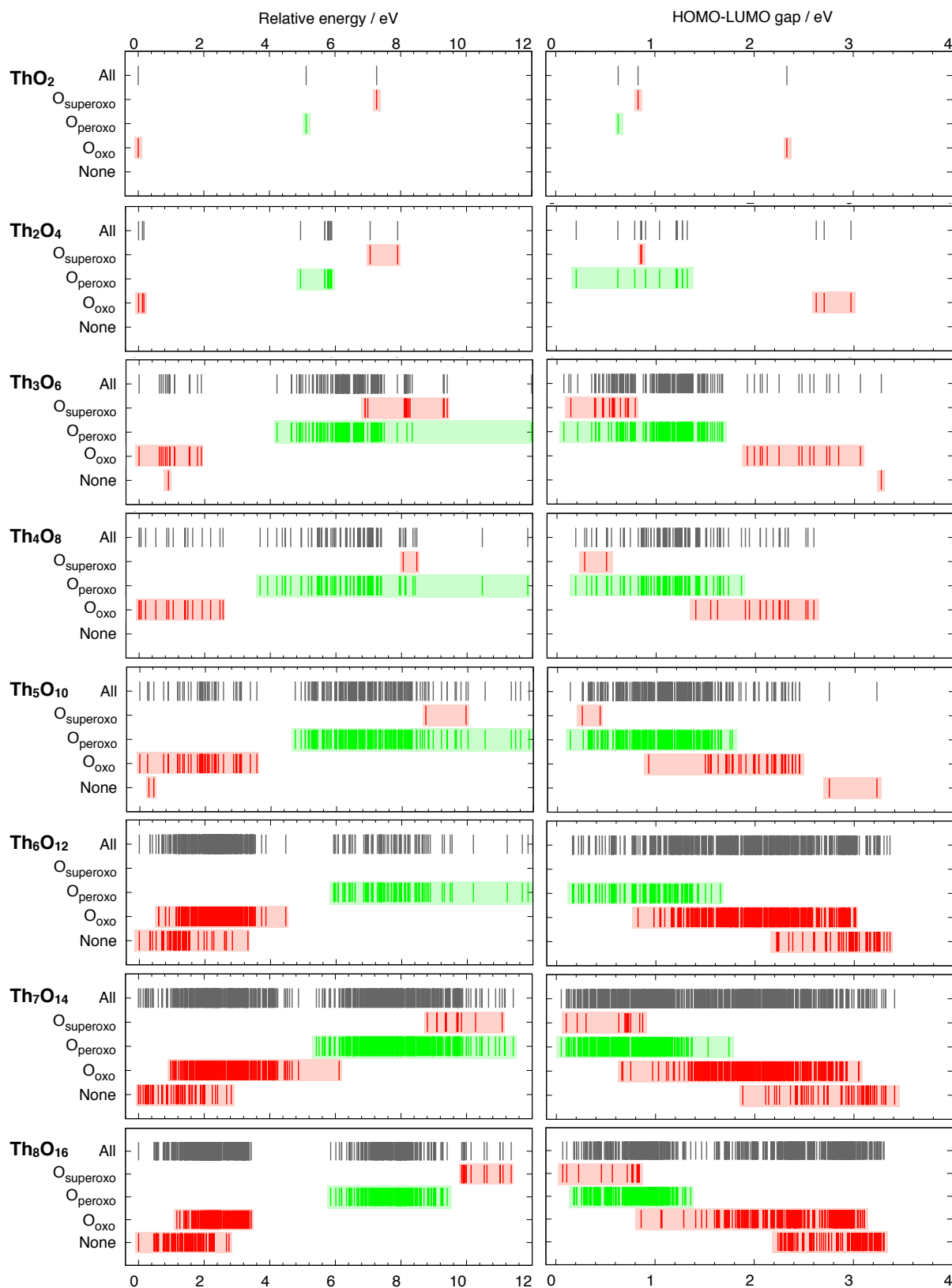


Fig. 3 Relative energy (Left) and HOMO-LUMO gap (right) for all structures belonging to the cluster series ranging from ThO_2 (top) to Th_8O_{16} (down). For each series, 'All' denotes the complete set of structures; ' $\text{O}_{\text{superoxo}}$ ' denotes the structures that contain at least one superoxo group (and may contain peroxo group(s) and/or terminal oxygen atom(s) as well); ' O_{peroxo} ' denotes the structures that contain at least one peroxo group (and may contain one or more terminal oxygen atoms); ' $\text{O}_{\text{terminal}}$ ' denotes the structures that contain at least one terminal oxygen atom (but no peroxo or superoxo group); and 'None' denotes the structures that do not contain any terminal oxygen atoms, peroxo and/or superoxo groups but only bridging oxygen atoms. Red denotes the structures for which the valence orbitals are dominated by oxygen contributions, while green denotes the structures for which the valence orbitals are dominated by thorium contributions. Grey has no specific meaning. The ensemble of structures used to produce this figure is shown in ESI† geometries-ThnO2n.zip

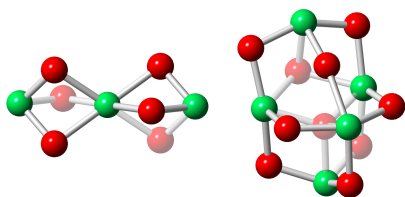


Fig. 4 Structure of the Th_3O_6 (left) and Th_5O_{10} (right) clusters not containing any oxo, peroxy or superoxy group

2.3 Correlation between geometry, relative energy and electronic structure

In order to establish correlations between the geometry, the relative energy and the electronic structure of the stoichiometric thorium dioxide clusters discussed in the previous section, we use a strategy similar to that employed for transition metal oxide clusters^{46–48} and metal- O_2 adducts.^{19,49–52} Namely, the relative energy and electronic structure of the clusters are analyzed with respect to the presence or the absence of superoxy groups (O_2^-), peroxy groups (O_2^{2-}), and/or terminal oxygen atoms (or oxo O^{2-} groups). For the electronic structure, the focus is put on (i) the composition of the highest occupied molecular orbital (HOMO) in terms of atomic orbitals (i.e. Th vs. O), and (ii) the HOMO-LUMO gap.

As expected, a clear correlation is observed between the presence or the absence of the different oxygen groups mentioned above, and the relative energy of the clusters (Figure 3). For instance, if the structure contains one or more superoxy groups, its total energy is at least 7 eV higher than that of the lowest energy structure (Figure 3, left). Notably, this energy difference tends to get bigger as the number of ThO_2 units contained in the cluster increases, reaching the value of 10 eV for the Th_8O_{16} series. In addition, every structure that contains at least one superoxy group appears to have its HOMO dominated by oxygen orbitals and localized on superoxy group. This observation holds whether the structure contains superoxy groups alone, or in combination with peroxy or oxo groups. Similarly, if the structure contains one or more peroxy groups (without any superoxy), its total energy is at least 3.5 eV higher than that of the lowest energy structure (Figure 3, left). This energy difference fluctuates between 3.5 eV and 6 eV across the series, and does not follow any specific trend. Interestingly, in the presence of peroxy groups, the HOMO is dominated by thorium orbitals, rather than oxygen orbitals. This observation is also true if the structure also contains additional one or more terminal oxygen atoms.

In the case of structures containing terminal oxygen oxo groups (but no superoxy or peroxy groups), the correlation is more complicated to analyze. As mentioned earlier, for all series ranging from ThO_2 to Th_5O_{10} , the lowest energy structure always contains at least one terminal oxygen atom, which is most likely a consequence of not having enough thorium atoms to bridge all the oxygen atoms. Hence, only the series ranging from Th_6O_{12} to Th_8O_{16} are relevant. For these three series, it is found that the total energy of the clusters containing one or more oxo groups is at least 0.5 eV higher than that of the lowest energy structure (Figure 3, left). Unlike the superoxy case, this energy difference increases

with the number of ThO_2 units, reaching the value of 1.2 eV for the Th_8O_{16} series. In addition, all the structures containing one or more oxo groups (but no superoxy or peroxy groups) have their HOMO dominated by oxygen orbitals located on the oxo groups.

It is noteworthy that the Th_nO_{2n} series with $n = 3$ and $n = 5$ both possess structures that do not contain any terminal oxo groups, 0.89 eV and 0.28 eV higher in energy than the lowest energy structure, respectively (Figure 4). For the Th_3O_6 cluster, the high energy structure appears to be rather constrained. Typically, all Th-O-Th angles are between 90° and 91° , when the angles in the low energy isomer are more obtuse (95° – 105°). Also, the average Th-Th bond distances appear to be smaller than for the lowest energy structure (i.e. 3.17 Å vs. 3.40 Å). This may explain why the structure with a terminal oxygen atom is favored. For the Th_5O_{10} cluster, the lowest energy structure exhibits high symmetry (C_{4v}), which may explain why it is so stable, despite having a terminal oxygen atom. This observation suggests that the ability of a cluster to achieve molecular symmetry (without significant constraints) can overcome the destabilizing effect of terminal oxygen atoms. This observation is supported by the conclusions of Knope *et al.* in their work on similar cluster.¹⁸

The correlation between the occurrence of different bonding patterns and the composition of the valence orbitals can be further extended to the oxidation state of the metal center, as can be seen from the electronic structure of the three ThO_2 isomers (Figure 5, and ESI†, Section S4.1 and Table S6). Indeed, these systems contain either two terminal oxygen atoms (or oxo groups), a peroxy group, or a superoxy group, and can thus be considered as simplified models to illustrate the correlation between bonding patterns and electronic structure. In isomer 1, the HOMO-LUMO gap is 2.33 eV, and the O-2p orbitals make the largest contribution to the valence orbitals, while the Th-7s and Th-6d orbitals make the largest contribution to the virtual orbitals. These features together with the computed dipole moment of 6.5 D, indicate charge transfer from the thorium to the oxygen atoms. This suggests that thorium is in the tetravalent oxidation state (+IV), and that thorium-oxygen interactions are highly ionic. For isomer 2, which contains a peroxy group, and which is 5.21 eV higher in energy than isomer 1, the HOMO-LUMO gap gets much smaller (0.63 eV). This is the sign of significant changes in the electronic structure, compared to isomer 1. Indeed, the Th-7s is now the orbital that makes the largest contribution to the valence orbitals, while the Th-5f and Th-6d orbitals make the largest contribution to the lower virtual orbitals. This suggests that thorium is in the divalent oxidation state (+II), with a $(7s)^2$ configuration. Finally, isomer 3, which is 7.27 eV higher in energy than isomer 1, and contains a superoxy group, has a HOMO-LUMO gap that is close to that of isomer 2 (0.83 eV), while its DOS exhibits notable differences: in addition to the contribution of the Th-7s orbital, the valence orbitals also show a sharp contribution of the O-2p orbitals. The low lying virtual orbitals, on the other hand, are still dominated by the Th-5f and Th-6d orbitals. Valence orbitals being mixed between the metal 7s and oxygen contributions indicated a more intricate electronic structure, and suggests that thorium is in the monovalent oxidation state (+I). Overall, the oxidation states of thorium highlighted above counter balance well

to the oxidation states expected for the different oxygen groups present in the three ThO_2 isomers. This result evidences the richness of the oxidation states available for thorium in the clusters studied in this work.

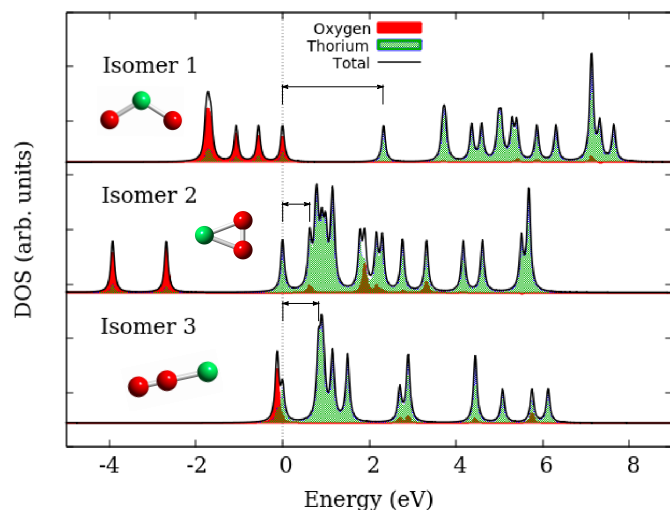


Fig. 5 Density of state for the three ThO_2 isomers (arrows indicate the HOMO-LUMO gaps)

In a nutshell, the relative energy of the thorium dioxide clusters is found to strongly depend on the presence or the absence of terminal oxygen atoms, peroxy groups and superoxy groups. Typically, as terminal oxygen atoms, peroxy and superoxy groups are 'added' to a structure, its relative energy is raised by at least 0.5 eV, 3.5 eV and 7 eV, respectively (assuming the cluster is large enough to accommodate all oxygen atoms and avoid the presence of terminal oxygen in the lowest energy structure). These bonding patterns are also found to correlate well with the composition of the HOMO: as soon as a cluster contains a superoxy group, its HOMO is dominated by the oxygen orbitals of the superoxy group, while in the presence of a peroxy group, the HOMO is dominated by thorium orbitals. For clusters containing terminal oxygen atoms solely or none of the aforementioned oxygen groups, the HOMO is always found to be dominated by oxygen orbitals. However, while it is localized on the terminal oxygen atom in the case of the oxo group, it is delocalized over all oxygen atoms when none of the aforementioned oxygen groups are present in the structure. Interestingly, the HOMO-LUMO gap of the clusters follows a different trend (Figure 3, right), as smaller gaps are obtained for the clusters containing superoxy and peroxy groups (~ 0 -1 eV and ~ 0 -2 eV, respectively), than for the clusters containing terminal oxygen atoms solely (~ 1 -3 eV) or none of the aforementioned patterns (~ 2 -3.5 eV). It is interesting that the aforementioned correlations hold throughout the entire series of clusters, i.e. from ThO_2 to Th_8O_{16} . This transferability is expected to be the consequence of keeping the ratio of thorium and oxygen atoms the same across the different cluster series. Hence, it is also expected to hold for larger clusters than the one studied in the present work. It should also be mentioned that this is the first-time such correlations are observed in actinide clusters. Interestingly, the energy ordering of the bonding motifs follows the

same trend as for transition metals,⁴⁶⁻⁴⁸ except for copper clusters, where the oxo group is found to increase the relative energy of the cluster more than the superoxy group. This result is reminiscent of that obtained from the analysis of the potential energy surface of TiO_2 .⁵³

2.4 ThO_2 clusters in chemistry

The previous sections shed light on the structural features that affect the relative energy and electronic structure of the stoichiometric thorium dioxide clusters, Th_nO_{2n} with $n = 1 - 8$. Besides their fundamental importance, these correlations are of great interest for applications ranging from energy storage, conversion and production,⁵⁴ to medical imaging⁵⁵, catalysis⁵⁶ or optoelectronics.⁵⁷ Indeed, these correlations can help design clusters with targeted electronic structure, and hence, improved performance. Yet, the desired electronic features may not be present in the lowest energy isomer, but in other isomers. In that context, this section discusses potential applications of thorium dioxide clusters, and potential synthetic strategies to ensure that a cluster contains the suitable electronic structure.

Throughout the series, the clusters that only contain bridging oxygen atoms (i.e. no oxo, peroxy or superoxy groups) show a HOMO dominated by oxygen orbitals, and a HOMO-LUMO gap that decreases from about 3.5 eV for Th_3O_6 to about 2 eV for Th_8O_{16} . In the presence of oxo or superoxy groups, the HOMO is found to be dominated by the $2p$ orbitals of the terminal oxygen atom. While the HOMO-LUMO gap of the clusters containing a superoxy group is fairly small (~ 0 -1 eV), that of the clusters containing an oxo group can take values from about 1 eV to about 3 eV. As highlighted in several recent reviews, such terminal features are highly desirable for applications involving charge dissociation (e.g. photonics and spintronics),^{54,57} and redox processes (e.g. catalysis, biomedical applications).^{55,56,58} Indeed, in metal oxide nanostructures, the valence electrons are generally localized on the terminal oxygen atoms (as evidenced in the present work as well), which makes these electrons readily accessible for redox reactions.^{55,56,58} Then, upon exciton dissociation, the hole is typically known to migrate towards the terminal oxygen atom(s) (i.e. towards the edge of the cluster) while the electron localizes on the metal centers (i.e. inner structure), hence leading to efficient charge separation.^{54,57} Unfortunately, such terminal features have been shown not to appear in the lowest energy structures; but making use of appropriate ligands or solvent effects, it is expected that higher energy structures containing these feature can be stabilized. To illustrate this statement, we take the particular example of the Th_6O_{12} cluster, which is closely related to the $[\text{Th}_6(\text{OH})_4(\text{O})_4(\text{O})_6]$ clusters previously studied, both theoretically and experimentally, by Knope *et al.*¹⁸ Despite having a different stoichiometry, the latter clusters hold similar features to the clusters investigated in the present work (e.g. terminal oxygen atoms, and thorium atoms bridged by oxygen atoms). Hence, we believe that the present correlations are likely to hold for this cluster as well, and that the strategy used to stabilize this cluster are likely to work for other stoichiometric clusters as well.

For the Th_6O_{12} structures studied in this work, the lowest en-

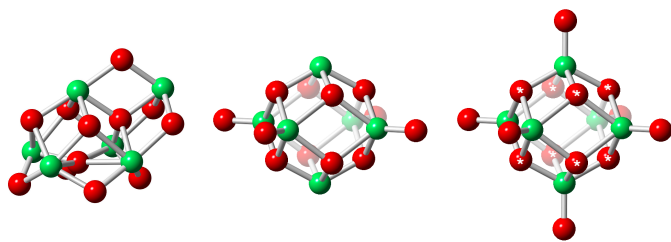


Fig. 6 Structure of the lowest energy Th_6O_{12} isomer this work (left), the Th_6O_{12} isomer by Shamov¹⁷ (middle), and the $[\text{Th}_6(\text{OH})_4(\text{O})_4(\text{O})_6]$ cluster core by Knope *et al.*¹⁸ (right - the white stars denote the oxygen atoms that can coordinate hydrogen atoms)

ergy isomer can be described as a square pyramid of thorium atoms bridged together by two oxygen atoms, and further capped (on one face of the pyramid) by another thorium atom and three oxygen atoms (Figure 6, left). This isomer has C_s symmetry, with Th-O bond distances typically ranging from 2.15 Å to 2.62 Å. Interestingly, the $[\text{Th}_6(\text{OH})_4(\text{O})_4(\text{O})_6]$ core of the clusters synthesized by Knope *et al.*¹⁸ is different. Yet it is reminiscent of another Th_6O_{12} isomer found 2.4 eV higher in energy than the lowest energy isomer. This isomer can be described as a rhombohedron with alternating thorium and oxygen atoms on the summits, and with four additional oxygen atoms further coordinating (in terminal position) the thorium atoms in the equatorial plane (Figure 6, middle), which was reported by Shamov as stable.¹⁷ This isomer has D_{4h} symmetry, with Th-O bond distances typically ranging from 1.91 Å to 2.45 Å. As expected from the presence of the terminal oxygen atoms, this cluster has a smaller HOMO-LUMO gap (2.05 eV) than the lowest energy structure (3.33 eV). The HOMO of both systems is dominated by O-2p orbitals, which are localized on the terminal oxygen atoms for the D_{4h} isomer, and delocalized over all oxygen atoms for the lowest energy structure. With respect to this D_{4h} isomer, the core of the clusters synthesized by Knope *et al.* contains two additional oxygen atoms in axial (terminal) position, while four of the eight bridging oxygen atoms are also coordinated by hydrogen atoms (Figure 6, right). This core is then decorated by either 12 formate, 12 acetate or 12 monochloroacetate groups, which further bridge every couple of neighboring thorium atoms.

The structural similarity between the core of the clusters by Knope *et al.* and that of the D_{4h} Th_6O_{12} isomer suggests that high energy stable isomers can be experimentally isolated by making use of appropriate ligands or solvent effects. Due to the presence of six terminal oxygen atoms, the cluster by Knope *et al.* is not expected to be the lowest energy one in gas phase. And indeed, the cluster with the same chemical formula as that by Knope *et al.*, but built using our Th_6O_{12} lowest energy isomer as core (ESI†, Section S5) is found 4.64 eV lower in energy. Hence, it is expected that the additional carboxylate groups, as well as hydrogen bonds with solvent (water), are responsible for the stabilization of the $[\text{Th}_6(\text{OH})_4(\text{O})_4(\text{O})_6]$ core by Knope *et al.* This example supports the idea that a stable isomer, yet not the lowest energy one, can be stabilized through ligand and/or solvent effects. Furthermore, as already mentioned by Knope *et al.*, it is strongly thought that this isomer in particular could be stabilized, because of its high

D_{4h} symmetry.¹⁸

3 Conclusions

To summarize, this work constitutes the very first systematic study of correlations between geometry, relative energy and electronic structure in stoichiometric thorium dioxide clusters. This was achieved by using first principle methods in combination with a new generation of geometry search algorithm, which screens homogeneously the potential energy surface, and allows us to unravel structural stability. Typically, the relative energy of thorium dioxide clusters ranging from ThO_2 and Th_8O_{16} appears to be driven by the presence or the absence of oxo, peroxy and/or superoxy groups. More precisely, it is found that the presence of peroxy and superoxy groups tends to increase the total energy of the system by about 3.5 eV and 7 eV, respectively, while the presence of terminal oxygen atoms increases it by about 0.5 eV. From the Th_5O_{10} series of clusters, it is found that these trends can be disrupted by the ability of the cluster to achieve high symmetry. Interestingly, these correlations can be taken advantage of to design clusters with desired geometric and electronic structure features. From the methodology point of view, the present work shows how powerful stochastic strategies can be to determine stable isomers. In combination with molecular dynamics approaches, this method could pave the way for a better understanding of nucleation and crystal growth, but also molecular transport, migration processes, and catalytic applications.

Conflicts of interest

There are no conflicts to declare.

Acknowledgements

This work was supported by the US Department of Energy through the Los Alamos National Laboratory. Los Alamos National Laboratory is operated by Triad National Security, LLC, for the National Nuclear Security Administration of U.S. Department of Energy (Contract No. 89233218NCA000001). The authors acknowledge the computing resources provided by Pacific Northwest National Laboratory (PNNL) on the supercomputer CASCADE and by LANL on the institutional computer cluster, Wolf. N.F.A. thanks LANL for funding through Seaborg postdoctoral fellowship awarded by the G. T. Seaborg Institute of Los Alamos National Laboratory (LANL). J. J. thanks LANL for funding through the Director's Postdoctoral Fellowship. P.Y. thanks the Heavy Element Chemistry program at LANL sponsored by the Division of Chemical Sciences, Geosciences, and Biosciences, Office of Sciences, U.S. Department of Energy.

Notes and references

- 1 H. Y. Choi and C. J. Park, *Annals of Nuclear Energy*, 2018, **116**, 171 – 176.
- 2 V. Jagannathan, *International Journal of Energy Research*, 2017, **42**, 117–133.
- 3 T. Yousefi, M. Torab-Mostaedi, H. G. Mobtaker and A. R. Keshkar, *Journal of Nuclear Materials*, 2016, **479**, 633 – 638.
- 4 J. Spino, H. S. Cruz, R. Jovani-Abril, R. Birtcher and C. Ferrero, *Journal of Nuclear Materials*, 2012, **422**, 27 – 44.

- 5 Y. Jiyang, W. Kan, Y. Songbo, J. Baoshan, S. Shifei, S. Gong, S. Rayman and R. Yangqiang, *Progress in Nuclear Energy*, 2004, **45**, 71 – 83.
- 6 M. S. Kazimi, *American Scientist*, 2003, **91**, 408–415.
- 7 M. Lung and O. Gremm, *Nuclear Engineering and Design*, 1998, **180**, 133 – 146.
- 8 J. Leduc, M. Frank, L. Jäijrgensen, D. Graf, A. Raauf and S. Mathur, *ACS Catalysis*, 2019, **9**, 4719–4741.
- 9 C. Walther and M. A. Denecke, *Chemical Reviews*, 2013, **113**, 995–1015.
- 10 L. Amidani, T. V. Plakhova, A. Y. Romanchuk, E. Gerber, S. Weiss, A. Efimenko, C. J. Sahle, S. M. Butorin, S. N. Kalmykov and K. O. Kvashnina, *Phys. Chem. Chem. Phys.*, 2019, **21**, 10635–10643.
- 11 G. Wang, E. Batista and P. Yang, *Phys. Chem. Chem. Phys.*, 2018, **20**, 17563–17573.
- 12 P. Burns, Y.-C. Chen, J.-W. Cheng, Y.-S. Ding, T. Han, S. Hickam, Z. Hou, S. Huang, R. Jones, X.-J. Kong, J.-L. Liu, L.-S. Long, T. Shima, M.-L. Tong, C. Wang, S. Wang, G.-Y. Yang, X. Yang, Y. Zhang, Z. Zhang, Z. Zheng, X.-Y. Zheng and Y.-Z. Zheng, in *Structure and Bonding*, Springer, Berlin, Heidelberg, 2017, vol. 173.
- 13 V. Tyrpekl, J.-F. Vigier, D. Manara, T. Wiss, O. D. Blanco and J. Somers, *Journal of Nuclear Materials*, 2015, **460**, 200 – 208.
- 14 R. Zhao, L. Wang, Z.-F. Chai and W.-Q. Shi, *RSC Adv.*, 2014, **4**, 52209–52214.
- 15 J. Qiu and P. C. Burns, *Chemical Reviews*, 2013, **113**, 1097–1120.
- 16 K. E. Knope, M. Vasiliu, D. A. Dixon and L. Soderholm, *Inorganic Chemistry*, 2012, **51**, 4239–4249.
- 17 G. A. Shamov, *Inorganic Chemistry*, 2012, **51**, 6507–6516.
- 18 K. E. Knope, R. E. Wilson, M. Vasiliu, D. A. Dixon and L. Soderholm, *Inorganic Chemistry*, 2011, **50**, 9696–9704.
- 19 H. Xiao, H.-S. Hu, W. H. E. Schwarz and J. Li, *The Journal of Physical Chemistry A*, 2010, **114**, 8837–8844.
- 20 A. S. Karakoti, P. Yang, W. Wang, V. Patel, A. Martinez, V. Shutthanandan, S. Seal and S. Thevuthasan, *The Journal of Physical Chemistry C*, 2018, **122**, 3582–3590.
- 21 S. T. Bromley, I. d. P. R. Moreira, K. M. Neyman and F. Illas, *Chemical Society Reviews*, 2009, **38**, 2657.
- 22 H.-J. Zhai, J. Džubler, J. Sauer and L.-S. Wang, *Journal of the American Chemical Society*, 2007, **129**, 13270–13276.
- 23 C. J. Pickard and R. J. Needs, *Journal of Physics: Condensed Matter*, 2011, **23**, 053201.
- 24 M. P. Kelley, J. Su, M. Urban, M. Luckey, E. R. Batista, P. Yang and J. C. Shafer, *Journal of the American Chemical Society*, 2017, **139**, 9901–9908.
- 25 L. Andrews, Y. Gong, B. Liang, V. E. Jackson, R. Flamerich, S. Li and D. A. Dixon, *The Journal of Physical Chemistry A*, 2011, **115**, 14407–14416.
- 26 V. E. Jackson, R. Craciun, D. A. Dixon, K. A. Peterson and W. A. de Jong, *The Journal of Physical Chemistry A*, 2008, **112**, 4095–4099.
- 27 B. O. Roos, P.-r. Malmqvist and L. Gagliardi, *Journal of the American Chemical Society*, 2006, **128**, 17000–17006.
- 28 J. Jung, M. Atanasov and F. Neese, *Inorganic Chemistry*, 2017, **56**, 8802–8816.
- 29 T. Nagata, J. W. J. Wu, M. Nakano, K. Ohshimo and F. Misaizu, *The Journal of Physical Chemistry C*, 2019, **123**, 16641–16650.
- 30 B. Dorado, M. Freyss, B. Amadon, M. Bertolus, G. Jomard and P. Garcia, *Journal of Physics: Condensed Matter*, 2013, **25**, 333201.
- 31 B. Dorado, G. Jomard, M. Freyss and M. Bertolus, *Phys. Rev. B*, 2010, **82**, 035114.
- 32 B. Dorado, B. Amadon, M. Freyss and M. Bertolus, *Phys. Rev. B*, 2009, **79**, 235125.
- 33 V. Kanchana, G. Vaitheeswaran, A. Svane and A. Delin, *Journal of Physics: Condensed Matter*, 2006, **18**, 9615.
- 34 N. F. Aguirre, S. Díaz-Tendero, P.-A. Hervieux, M. Alcamí and F. Martín, *Journal of Chemical Theory and Computation*, 2017, **13**, 992–1009.
- 35 W. R. Wadt, *Journal of the American Chemical Society*, 1981, **103**, 6053–6057.
- 36 G. M. Kibler, T. F. Lyon, M. J. Linevski and V. J. DeSantis, *Refractory Material Research*, Air force materials laboratory - research and technology division - air force systems command - wright-patterson air force base, ohio, usa technical report, 1964.
- 37 S. D. Gabelnick, G. T. Reedy and M. G. Chasanov, *The Journal of Chemical Physics*, 1974, **60**, 1167–1171.
- 38 M. Zhou and L. Andrews, *The Journal of Chemical Physics*, 1999, **111**, 11044–11049.
- 39 L. Andrews, M. Zhou, B. Liang, J. Li and B. E. Bursten, *Journal of the American Chemical Society*, 2000, **122**, 11440–11449.
- 40 A. Kovács and R. J. Konings, *The Journal of Physical Chemistry A*, 2011, **115**, 6646–6656.
- 41 K. G. Dyall, *Molecular Physics*, 1999, **96**, 511–518.
- 42 I. A. Sarsari, S. J. Hashemifar and H. Salamati, *Journal of Physics: Condensed Matter*, 2012, **24**, 505502.
- 43 R. D. Parra and H. H. Farrell, *The Journal of Physical Chemistry C*, 2009, **113**, 4786–4791.
- 44 B. Wang, X. Wang and J. Zhao, *The Journal of Physical Chemistry C*, 2010, **114**, 5741–5744.
- 45 D. Hudry, C. Apostolidis, O. Walter, T. Gouder, E. Courtois, C. Kăijbel and D. Meyer, *Chemistry âĀŞ A European Journal*, 2013, **19**, 5297–5305.
- 46 E. L. Uzunova, H. Mikosch and G. S. Nikolov, *The Journal of Chemical Physics*, 2008, **128**, 094307.
- 47 G. L. Gutsev, B. K. Rao and P. Jena, *The Journal of Physical Chemistry A*, 2000, **104**, 11961–11971.
- 48 G. L. Gutsev, K. V. Bozhenko, L. G. Gutsev, A. N. Utenyshev and S. M. Aldoshin, *The Journal of Physical Chemistry A*, 2017, **121**, 845–854.
- 49 A. Singha, P. K. Das and A. Dey, *Inorganic Chemistry*, 0, **0**, null.
- 50 C. J. Cramer, W. B. Tolman, K. H. Theopold and A. L. Rheingold, *Proceedings of the National Academy of Sciences*, 2003,

- 100, 3635–3640.
- 51 P. L. Holland, *Dalton Transactions*, 2010, **39**, 5415.
- 52 X.-X. Li, K.-B. Cho and W. Nam, *Inorganic Chemistry Frontiers*, 2019.
- 53 C.-K. Lin, J. Li, Z. Tu, X. Li, M. Hayashi and S. H. Lin, *RSC Advances*, 2011, **1**, 1228.
- 54 J. Wang, Y. Cui and D. Wang, *Advanced Materials*, 2019, **31**, 1801993.
- 55 L. Yang, Z. Zhou, J. Song and X. Chen, *Chem. Soc. Rev.*, 2019, **48**, 5140–5176.
- 56 A. Akbari, M. Amini, A. Tarassoli, B. Eftekhari-Sis, N. Ghasemian and E. Jabbari, *Nano-Structures & Nano-Objects*, 2018, **14**, 19 – 48.
- 57 X. Yu, T. J. Marks and A. Facchetti, *Nature Materials*, 2016, **15**, 383.
- 58 D. Pla and M. Gãşmez, *ACS Catalysis*, 2016, **6**, 3537–3552.